BMC Women's Health

RESEARCH

Open Access

Unraveling the fibrotic microenvironment in intrauterine adhesions through integrated metabolomics and proteomics

Shuhan He[1†], Hui Yuan[1†], Xingping Zhao[1,2], Enuo Peng[1], Dabao Xu[1*] and Aiqian Zhang[1*]

Abstract

Background Intrauterine adhesions (IUA) result from endometrial basal layer injury, leading to fibrous tissue formation and impaired fertility. Current treatments fail to fully reverse the fibrotic microenvironment. This study aimed to elucidate molecular mechanisms underlying IUA-associated fibrosis through integrated metabolomics and proteomics.

Methods Fibrotic tissues from 35 moderate-to-severe IUA patients and normal endometrial samples from 20 controls were collected during hysteroscopy. Metabolomic profiling was performed using UPLC-MS, and proteomic analysis using label-free quantitative mass spectrometry. Differential metabolites (DEMs) and proteins (DEPs) were identified via OPLS-DA and statistical criteria (VIP > 1, $P < 0.05$ for DEMs; FDR-adjusted $P < 0.05$, FC ≥ 2 or ≤ 0.5 for DEPs). KEGG enrichment and integrated correlation analyses were conducted to explore pathway alterations and metabolite-protein interactions.

Results A total of 565 DEMs were identified, primarily lipids, organic acids, and organooxygen compounds. KEGG enrichment revealed significant alterations in carbohydrate and amino acid metabolism pathways, with downregulation of TCA cycle intermediates and upregulation of glucose-6-phosphate, arginine, and methionine sulfoxide. Proteomics identified 2763 DEPs, with up-regulated proteins enriched in focal adhesion and ECM-receptor interaction pathways, and down-regulated proteins in DNA replication and complement cascades. Integrative analysis showed that carbohydrate and amino acid metabolism-related DEMs correlated negatively with fibrosis-related DEPs (e.g., collagens, TGF-β-related proteins), while focal adhesion-related DEPs correlated positively with fibrosis markers. Notably, fumarate showed strong negative correlations with COL18A1 (r=-0.71) and positive correlation with E-cadherin ($r = 0.61$).

Conclusions This multi-omics study reveals that metabolic reprogramming, particularly involving glycolysis and amino acid metabolism, is closely associated with activation of the integrin-focal adhesion signaling pathway in IUA

†Shuhan He and Hui Yuan contributed equally to this work.

*Correspondence:
Dabao Xu
dabaoxu2022@163.com
Aiqian Zhang
Zhangaiqian1112@126.com

Full list of author information is available at the end of the article

fibrosis. These findings provide new insights into potential therapeutic targets for endometrial repair and fertility preservation.

Keywords Intrauterine adhesions, Fibrosis, Metabolomics, Proteomics

Introduction

Intrauterine Adhesions (IUA), also known as Asherman's Syndrome, encompasses a range of fibrotic gynecological conditions caused by injury to the endometrial basal layer [1]. Such injuries commonly result from pregnancy-related procedures like induced abortion or curettage, postpartum hemorrhage, or from non-gravid factors including intrauterine infection and endometrial tuberculosis [1, 2]. IUA is a significant cause of infertility and, even when pregnancy is achieved, carries substantial risks for serious obstetric complications such as missed abortion, placental adhesion, and placenta accreta, thereby posing a significant challenge to women's reproductive health [3]. Epidemiological studies that the prevalence of IUA among individuals with impaired fertility ranges from 2.8% to 45.5% [4]. The incidence of IUA is reported at 37.6% following post-abortion curettage and 40.0% after repeat curettage for incomplete abortion [5]. With the comprehensive implementation of China's "three-child" policy, the demand for protecting the reproductive health of women pursuing additional children has increased, making the elucidation of IUA pathogenesis and the development of effective therapeutic strategies critically important.

Transcervical Resection of Adhesions (TCRA) is the established gold standard for treating IUA, designed to resect or separate intrauterine fibrous adhesions under direct vision to restore normal uterine anatomy and volume [6]. However, TCRA only addresses anatomical obstruction without fundamentally reversing the underlying profibrotic microenvironment and the associated failure of endometrial regeneration in the damaged area [7]. This leads to high postoperative recurrence rates, reported as > 1/3 for mild-to-moderate IUA and exceeding 2/3 for severe cases [8]. To address this challenge, various adjuvant therapies have emerged, including physical barriers (e.g., Foley balloon catheter [9], intrauterine device [10], sodium hyaluronate gel [11]), biomaterials (e.g., fresh amniotic membrane grafts [12]), hormonal support (estrogen-progesterone sequential therapy [13]), and even advanced regenerative medicine approaches (e.g., stem cell transplantation [14]). While these methods demonstrate some efficacy in preventing short-term re-adhesion and partially encouraging endometrial coverage, they largely constitute passive or supportive measures that do not directly target the core molecular drivers of fibrosis, leading to limited and often unpredictable outcomes. This highlights the urgent need to understand IUA pathogenesis at its molecular and cellular origins.

Recent metabolomic studies have sought to identify mechanisms and therapeutic targets for IUA. Liu et al. pioneered the use of untargeted metabolomics comparing endometrial tissue from IUA patients and healthy women, identifying significant alterations in metabolites including diacylcarnitine, flusilazole, and lysyl-hydroxyproline [15]. Furthermore, a GC-TOF-MS-based serum metabolomics study found that *Prunella vulgaris* oil (PVO) significantly ameliorated intrauterine inflammation and fibrosis in a rat IUA model, primarily by modulating amino acid and derivative metabolism to rebalance related pathologies and control energy metabolism [16]. Concurrently, Halofuginone, an inhibitor of prolyl-tRNA synthetase, has demonstrated significant efficacy in multiple organ fibrosis models by specifically interfering with TGF-β/Smad pathway activation [17]. These findings strongly suggest that IUA progression involves profound metabolic reprogramming, intricately linked with protein signaling networks.

This study aims to systematically analyze clinically collected endometrial tissues from IUA patients and controls using label-free quantitative proteomics combined with UPLC-MS metabolomics. We will comprehensively identify differentially expressed proteins (DEPs) and differentially expressed metabolites (DEMs) in IUA endometrium. Integrated correlation analysis of the proteomic and metabolomic datasets will be performed to construct a protein-metabolite interaction network, thereby revealing significantly altered biological processes and pathways at both the protein and metabolite levels in IUA.

Method

Study subjects

The study protocol was developed and implemented with the support of the Third Xiangya Hospital of Central South University., while sample collection was additionally supported by the hospital's Department of Gynecology. From January 2022 to October 2023, a total of 55 intraoperative fibrotic tissue and normal endometrial samples were collected from IUA and non-IUA patients. The study protocol was approved by the Ethics Committee of the Third Xiangya Hospital of Central South University (Approval No. Kua 24558).

Inclusion criteria for the IUA group were: (1) diagnosed with moderate-to-severe IUA (American Fertility Society score (AFS) ≥ 5); (2) age 20–45 years; (3) presented with reduced menstrual volume and had

fertility requirements; (4) samples collected during the early proliferative phase (3–7 days after menstruation) whenever identifiable menstrual cycles permitted. For patients with irregular cycles, phase was estimated based on menstrual history and confirmed by endometrial dating when feasible. Inclusion criteria for the Control group were: patients aged 20–45 years (with tubal factor infertility or uterine cesarean scar diverticulum) who underwent hysteroscopy or combined hysteroscopy-laparoscopy during the same period (3–7 days after menstruation) and were pathologically confirmed to have no endometrial lesions.

Exclusion criteria for both groups were: (1) cervical or endometrial pathologies; (2) congenital uterine malformations; (3) pelvic tuberculosis; (4) co-existing uterine fibroids, adenomyosis, or endometrial polyps; (5) endocrine abnormalities; (6) severe systemic diseases.

All 55 tissue samples collected (35 from the IUA group and 20 from the control group) were subjected to both metabolomics and proteomics analyses. Immediately after hysteroscopic collection, each tissue specimen was divided into two aliquots under sterile conditions: one aliquot was promptly processed for metabolomic extraction to minimize metabolite degradation, and the other was snap-frozen in liquid nitrogen and stored at − 80 °C until proteomic analysis. Thus, identical tissue samples from each participant were used across both omics' platforms, ensuring direct comparability between the metabolomic and proteomic datasets.

Tissue sample collection and processing

During hysteroscopy, fibrotic tissue samples were selectively obtained from the central core of the intrauterine adhesions under direct visualization, carefully avoiding the marginal transitional zones to ensure predominant representation of the fibrotic core. For the control group, normal endometrial tissue was collected from a standardized location on the posterior wall of the uterine corpus, approximately 1–2 cm above the internal os, during the proliferative phase (days 7–10 of the menstrual cycle). Immediately after collection, each tissue specimen was divided into two equal aliquots under sterile conditions. One aliquot was promptly transferred to pre-cooled extraction solvent for metabolomic analysis to minimize metabolite degradation. The other aliquot was snap-frozen in liquid nitrogen within 2 min and stored at − 80 °C until proteomic analysis. Importantly, both aliquots originated from the exact same tissue fragment obtained from each participant, ensuring direct comparability between the metabolomic and proteomic datasets.

Metabolomics analysis

Tissue samples were precisely weighed, and metabolites were extracted with a pre-cooled methanol-acetonitrile-water solution (2:2:1, v/v). The samples were then vortex-mixed, sonicated in an ice bath, incubated at -20 °C, and centrifuged at high speed, after which the supernatant was collected and vacuum-dried before instrumental analysis. To monitor analytical stability and reproducibility, a quality control sample was prepared by combining equal aliquots from all test samples.

Chromatographic separation was performed on an ACQUITY UPLC® HSS T3 column using 0.1% formic acid in water (A) and 100% acetonitrile (B) as mobile phases under a gradient elution program at a total flow rate of 0.3 mL/min. Mass spectrometric detection was conducted on a Q-Exactive Plus mass spectrometer equipped with an electrospray ionization source, acquiring data in both positive and negative ion modes. The full scan resolution was set to 70,000, covering a mass range of m/z 70-1050.

Raw data were processed using R software (version 4.0.3). Data were first Pareto-scaled, followed by Principal Component Analysis to observe overall distribution. Orthogonal Partial Least Squares-Discriminant Analysis was employed to maximize group separation. Model reliability and predictive ability were assessed via a 200-time permutation test to prevent overfitting. Differential metabolites were screened based on a variable importance in projection value > 1.0 in the OPLS-DA model and a P-value < 0.05 from a two-tailed Student's t-test. Significantly altered pathways were identified using the Kyoto Encyclopedia of Genes and Genomes database via Fisher's exact test, with $P < 0.05$ considered statistically significant.

Proteomics analysis

Tissue samples were ground in liquid nitrogen, and total protein was extracted using SDT lysis buffer and quantified via the BCA assay. After reduction with dithiothreitol and alkylation with iodoacetamide, equal protein aliquots were digested with trypsin using the Filter-Aided Sample Preparation method on 10 kD ultrafiltration devices for 16–18 h. The resulting peptides were desalted using C18 Cartridges, lyophilized, reconstituted in 0.1% formic acid, and quantified.

Peptide separation was performed using a nano-liquid chromatography system with a linear gradient elution over 80 min, employing 0.1% formic acid in water and 80% acetonitrile containing 0.1% formic acid as mobile phases. The separated peptides were analyzed using an Orbitrap Astral mass spectrometer operating in data-independent acquisition mode. Full MS resolution was set to 240,000 and MS/MS resolution to 80,000. The acquired DIA data were processed and quantified using DIA-NN software against the UniProt human proteome database (downloaded July 2023, containing

207,981 entries) for protein identification and relative quantification.

Statistical analysis

For baseline clinical data, continuous variables conforming to a normal distribution were compared using the t-test and are presented as mean ± standard deviation; categorical data were analyzed using the Chi-square test. All statistical analyses were performed using SPSS 26.0 software, with $P < 0.05$ considered statistically significant. In omics data analysis, in addition to the specific multivariate statistical methods mentioned above, differential proteins were screened using a combination of fold change (FC) analysis and statistical testing. Specifically, proteins with FC ≥ 2.0 or ≤ 0.5 and a false discovery rate (FDR)-adjusted *P-value* < 0.05 (calculated using the Benjamini-Hochberg method) were considered significantly differentially expressed. For metabolomics data, differential metabolites were initially identified based on VIP > 1 and Student's t-test $P < 0.05$. For the subsequent integrated correlation analysis between DEMs and DEPs, Pearson correlation P-values were adjusted using the Benjamini-Hochberg method to control for multiple testing. Adjusted $P < 0.05$ was considered statistically significant in the correlation analysis. Pearson correlation analysis between significantly differential metabolites and proteins was performed using the psych package in R (version 4.3.3), with P-values adjusted using the Benjamini-Hochberg method. Results were visualized using the corrplot package.

Result

Characteristics of the study subjects

The IUA group consisted of 35 participants, with a mean (± SD) age of 32.72 ± 4.41 years, a BMI of 22.20 ± 3.53 kg/m², and an IUA AFS score of 9.92 ± 1.57. The control group comprised 20 participants, with a mean age of 30.90 ± 4.11 years and a BMI of 21.76 ± 3.45 kg/m². No statistically significant differences were observed between the two groups in terms of age, parity, height, weight, or BMI ($P > 0.05$). However, the IUA group had significantly higher gravidity (3.31 ± 1.55 vs. 1.55 ± 1.36, $P < 0.05$) and a greater number of prior intrauterine procedures (2.47 ± 1.25 vs. 0.40 ± 0.60, $P < 0.05$) compared to the control group (Table 1).

Screening of DEMs

An OPLS-DA model was constructed to explore metabolite expression differences between the IUA and control groups. The score plot showed clear separation between the two groups (Fig. 1A). Permutation tests confirmed model validity (positive ion mode: RY2 = 0.906, Q2 = 0.604; negative ion mode: RY2 = 0.997, Q2 = 0.667) (Fig. 1B). Using VIP > 1 and $P < 0.05$ as criteria, a total of 565 DEMs were identified, including 345 in positive ion mode and 220 in negative ion mode. Among these, 212 DEMs were up-regulated and 353 were down-regulated in the IUA group (Fig. 1C). The DEMs were predominantly lipids and lipid-like molecules, followed by organic acids and derivatives, and organooxygen compounds (Fig. 1D).

KEGG pathway enrichment analysis of DEMs

KEGG pathway enrichment analysis revealed that the DEMs were primarily enriched in pathways related to carbohydrate metabolism and amino acid metabolism (Fig. 2A and B). Given this enrichment, we further investigated the DEMs associated with these metabolic processes. The analysis revealed an overall down-regulation trend for carbohydrate metabolism-related DEMs in the IUA group (Fig. 2C). Similarly, amino acid metabolism-related DEMs were mostly down-regulated in the IUA group (Fig. 2D). In contrast, specific amino acids and derivatives, including arginine, lysine, tyrosine, and methionine sulfoxide, were significantly up-regulated.

Proteomics multivariate statistical analysis and screening of DEPs

An OPLS-DA model was employed to construct a relationship model between protein expression and sample categories and to predict sample classification. The model results showed tight clustering of samples within groups and clear separation between groups, verifying the model's reliability (Fig. 3A). A permutation test (RY2 = 0.991, Q2 = 0.921) indicated good model fit and predictive ability (Fig. 3B).

For identifying significant DEPs, a student's t-test combined with FC analysis was used, followed by FDR correction using the Benjamini-Hochberg method. Proteins with an FDR-adjusted *P-value* < 0.05 and FC ≥ 2.0 or ≤ 0.5 were considered statistically significant. Using these stringent criteria, a total of 2763 DEPs were identified between the IUA and control groups, of which 801 were up-regulated and 1962 were down-regulated

Table 1 Characteristics of the study subjects

	Age	Gravidity	Parity	Procedures Counts	Height (m)	Weight (kg)	BMI	AFS score
IUA group	32.72 ± 4.41	3.31 ± 1.55	0.86 ± 0.87	2.47 ± 1.25	1.58 ± 0.06	55.61 ± 9.66	22.20 ± 3.53	9.92 ± 1.57
Control group	30.90 ± 4.11	1.55 ± 1.36	1.00 ± 0.92	0.40 ± 0.60	1.59 ± 0.05	55.10 ± 7.92	21.76 ± 3.45	/
P-value	0.90	<0.05	0.56	<0.05	0.72	0.677	0.78	/

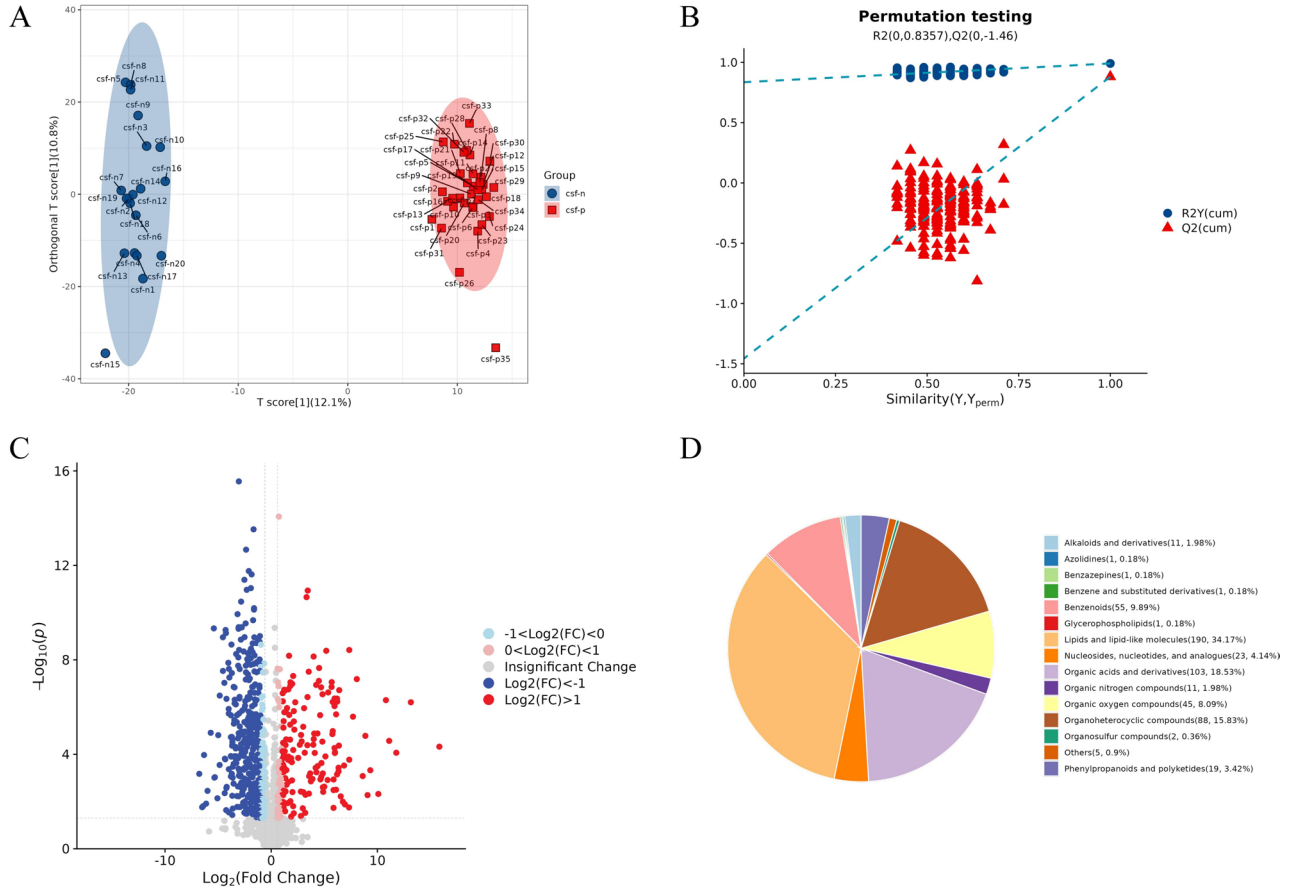

Fig. 1 Identification of differentially expressed metabolites (DEMs) in IUA vs. control groups. **A** OPLS-DA score plot showing separation between IUA (red) and control (blue) groups. **B** Permutation test (200 iterations) confirming model validity (positive mode: $R^2Y = 0.906$, $Q^2 = 0.604$; negative mode: $R^2Y = 0.997$, $Q^2 = 0.667$). **C** Volcano plot of DEMs. Red: up-regulated ($n = 212$); blue: down-regulated ($n = 353$); gray: not significant. **D** Classification of identified DEMs by chemical category

in the IUA group. A volcano plot visually displays these DEPs between the two groups (Fig. 3C). A volcano plot visually displays these DEPs between the two groups (Fig. 3C). To compare fibrotic expression differences, a subset of fibrosis-related proteins was selected from the DEPs, including collagens (COL5A1, COL4A5, COL4A6, COL18A1, COL4A1, COL1A1, COL4A2, COL1A2, COL5A2), TGF-β-related proteins (TGF-βig-h3, TGF-β1, TGF-β1|1), matrix metalloproteinases (MMP2, MMP19), laminins (LAMC1, LAMA2, LAMB2, LAMA4, LAMA3), and E-cadherin (CDH1). The results showed an overall up-regulation of these fibrosis-related DEPs in the IUA group and down-regulation in the control group (Fig. 3D).

KEGG pathway enrichment analysis of DEPs

GO enrichment analysis showed that DEPs were significantly enriched in Biological Processes related to cellular component organization, cytoskeleton organization, and cell adhesion; in Cellular Components including extracellular matrix and collagen-containing extracellular matrix; and in Molecular Functions including structural molecule activity and cytoskeletal protein binding (Fig. 4A and C). KEGG pathway enrichment results indicated that up-regulated DEPs were primarily enriched in Focal adhesion, ECM-receptor interaction, Dilated cardiomyopathy, Hypertrophic cardiomyopathy, and Arrhythmogenic right ventricular cardiomyopathy pathways. Down-regulated DEPs were mainly enriched in DNA replication, Complement and coagulation cascades, Cell cycle, and other glycosylation-related pathways (Fig. 4D). Proteins involved in focal adhesion including focal adhesion complex proteins (TLN1, TLN2, PTK2, VCL, PXN) and integrins (ITGB1, ITGA1, ITGB6, ITGA5, ITGA3, ITGA7, ITGA11, ITGA9, ITGA8, ITGB4, ITGB1BP2, etc.), were predominantly up-regulated in the IUA group (Fig. 4E).

Relationship between Glucose/Amino Acid Metabolism and IUA Fibrosis

Pearson correlation analysis was performed to examine the relationship between metabolism-related DEMs

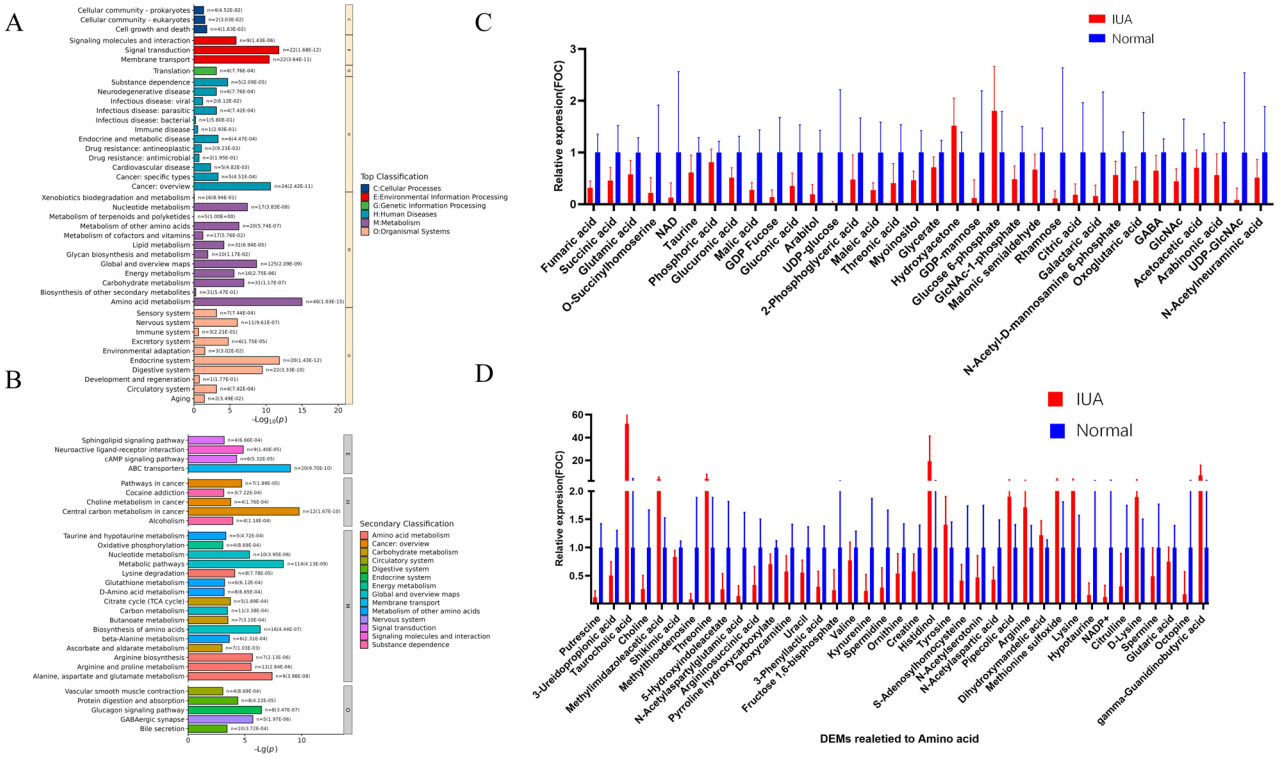

Fig. 2 KEGG pathway enrichment and expression patterns of metabolism-related DEMs. **A** Level 1 and (**B**) Level 2 KEGG pathway classifications of DEMs. Heatmaps showing expression levels of (**C**) carbohydrate metabolism-related and (**D**) amino acid metabolism-related DEMs in IUA vs. control groups. Color scale represents normalized abundance

and fibrosis-related DEPs. The results showed an overall negative correlation between carbohydrate and amino acid metabolism-related DEMs and fibrosis-related DEPs (Fig. 5A and B). Analysis of carbohydrate metabolism-related DEMs versus fibrosis-related DEPs showed that TCA cycle intermediates, such as fumarate, correlated negatively with fibrillar collagens (COL5A1, COL4A5, COL4A6, COL18A1, COL4A1, COL1A1, COL4A2, COL1A2, COL5A2), TGF-β-related DEPs, matrix metalloproteinases (MMP2, MMP19), and laminins (LAMA2, LAMB2, LAMA4, LAMA3), but positively with CDH1. Notably, fumarate showed a strong negative correlation with COL18A1 (r = -0.70701) and a strong positive correlation with E-cadherin (CDH1; r = 0.606022). Conversely, glucose-6-phosphate showed positive correlations with the fibrillar collagens, TGF-β-related DEPs, and matrix metalloproteinases, and a negative correlation with CDH1, although these correlations were relatively weak.

Relationship between focal adhesion signaling pathway and glucose/amino acid metabolism

Correlation analysis revealed an overall positive correlation between focal adhesion-related DEPs and fibrosis-related DEPs (Fig. 5C). For instance, Vinculin (VCL) correlated positively with fibrillar collagens (COL5A1, COL4A5, COL4A6, COL18A1, COL4A1, COL1A1, COL4A2, COL1A2, COL5A2), TGF-β-related DEPs, matrix metalloproteinases (MMP2, MMP19), and laminins (LAMA2, LAMB2, LAMA4, LAMA3), but negatively with CDH1. VCL showed a strong positive correlation with LAMC1 (r = 0.854745) and a moderate negative correlation with E-cadherin (CDH1; r = -0.59963).

Further analysis showed that the majority of glucose and amino acid metabolism-related DEMs correlated negatively with focal adhesion-related DEPs (Fig. 5D and E). Notably, fumarate correlated negatively with VCL (r = -0.65), putrescine correlated negatively with VCL (r = -0.66), while arginine showed a weak positive correlation with VCL (r = 0.36).

Discussion

IUA, which cause infertility, missed abortion, and other adverse pregnancy outcomes, represent a significant challenge in the field of female fertility preservation. Although clinical strategies such as hysteroscopic adhesiolysis, physical barrier isolation, and sequential estrogen-progesterone therapy have partially controlled adhesion recurrence and promoted endometrial repair, the long-term prognosis of IUA remains unsatisfactory. The fundamental reason lies in the incomplete understanding of the molecular mechanisms driving fibrosis.

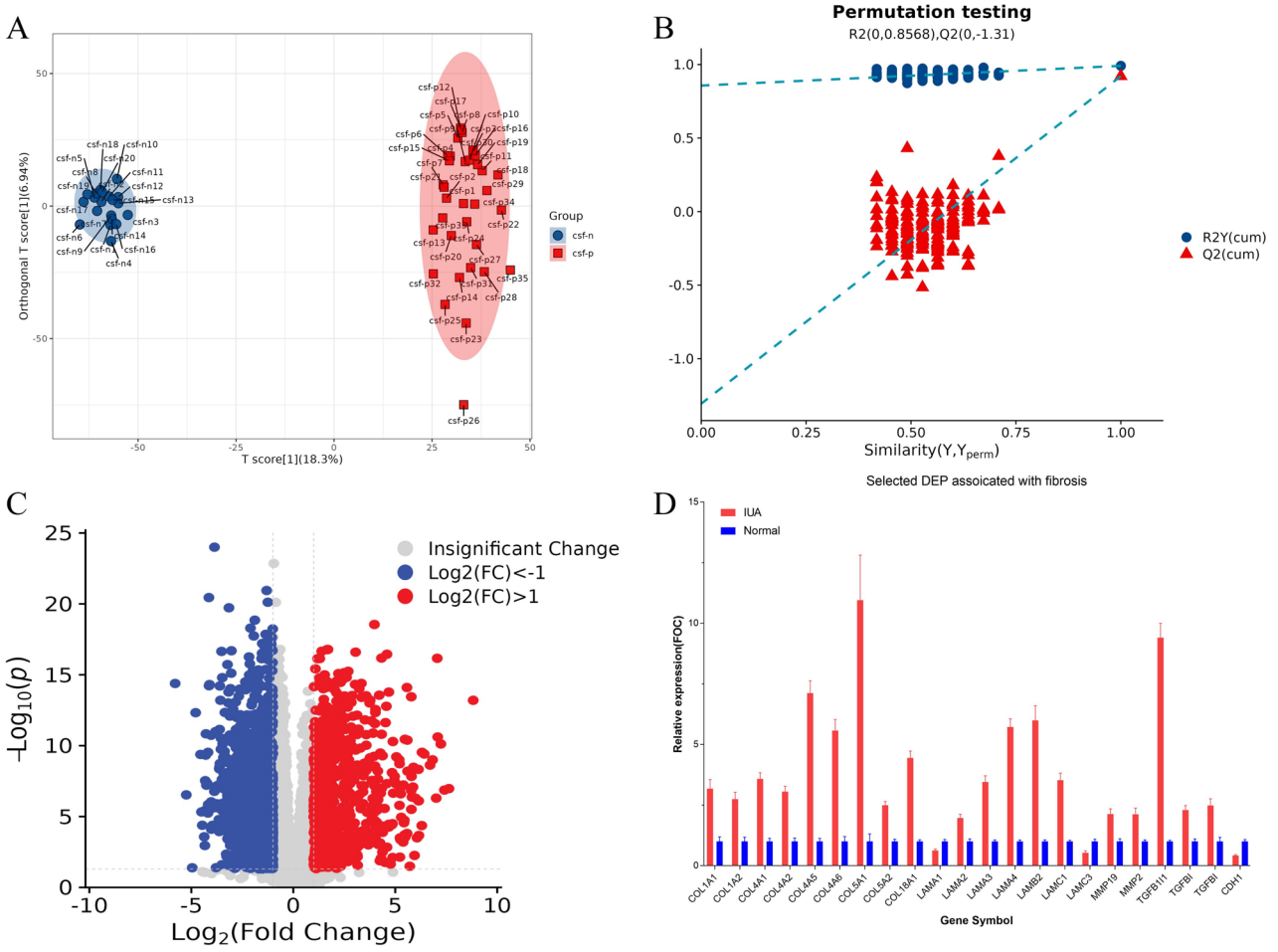

Fig. 3 Identification of differentially expressed proteins (DEPs) in IUA vs. control groups. **A** OPLS-DA score plot and **(B)** permutation test ($R^2Y=0.991$, $Q^2=0.921$) confirming model validity. **C** Volcano plot of DEPs. Red: up-regulated ($n=801$); blue: down-regulated ($n=1962$); gray: not significant. **D** Expression levels of selected fibrosis-related DEPs in IUA vs. control groups

Recent evidence indicates metabolic reprogramming participates broadly in diverse tissue fibrotic processes [18], offering a new perspective for addressing IUA. This study integrated metabolomics and proteomics analyses to systematically investigate the associations between metabolic alterations, focal adhesion signaling, and fibrosis in IUA, providing a foundation for hypothesis generation regarding potential mechanistic interactions.

Metabolomics results indicated significant amino acid metabolic disturbances in IUA patients. This study found a significant upregulation of methionine sulfoxide in the IUA group, alongside downregulated expression of ornithine and its metabolite glutamine. Studies have shown that methionine can be oxidized by reactive oxygen species to form methionine sulfoxide [18], while the ornithine cycle participates in ammonia clearance and can contribute to antioxidant defense through the generation of glutamine [19]. These findings imply localized oxidative stress and reduced antioxidant capacity in the endometrial cells of IUA patients, potentially aggravating endometrial injury and fibrosis. Concurrently, this study observed a significant upregulation of arginine and a significant downregulation of one of its metabolites, spermidine, in the IUA group. Although arginine supplementation has been shown to improve thin endometrium [20], it plays a dual role in the context of fibrosis: arginine is converted to proline and hydroxyproline, directly supporting collagen synthesis and stabilization [21]; while a decline in its metabolite spermidine may compromise autophagy induction, favoring abnormal extracellular matrix deposition [22]. Li et al. demonstrated that lung fibroblast proliferation was significantly suppressed under arginine-free culture, indicating that arginine is associated with fibroblast activation *in vitro* [23].

Simultaneously, the glucose metabolic pathway in IUA exhibited significant alterations, characterized by upregulated glucose-6-phosphate expression and significant decreases in key TCA cycle intermediates such as succinate, fumarate, and citrate. These changes are consistent with a shift in cellular energy metabolism from oxidative

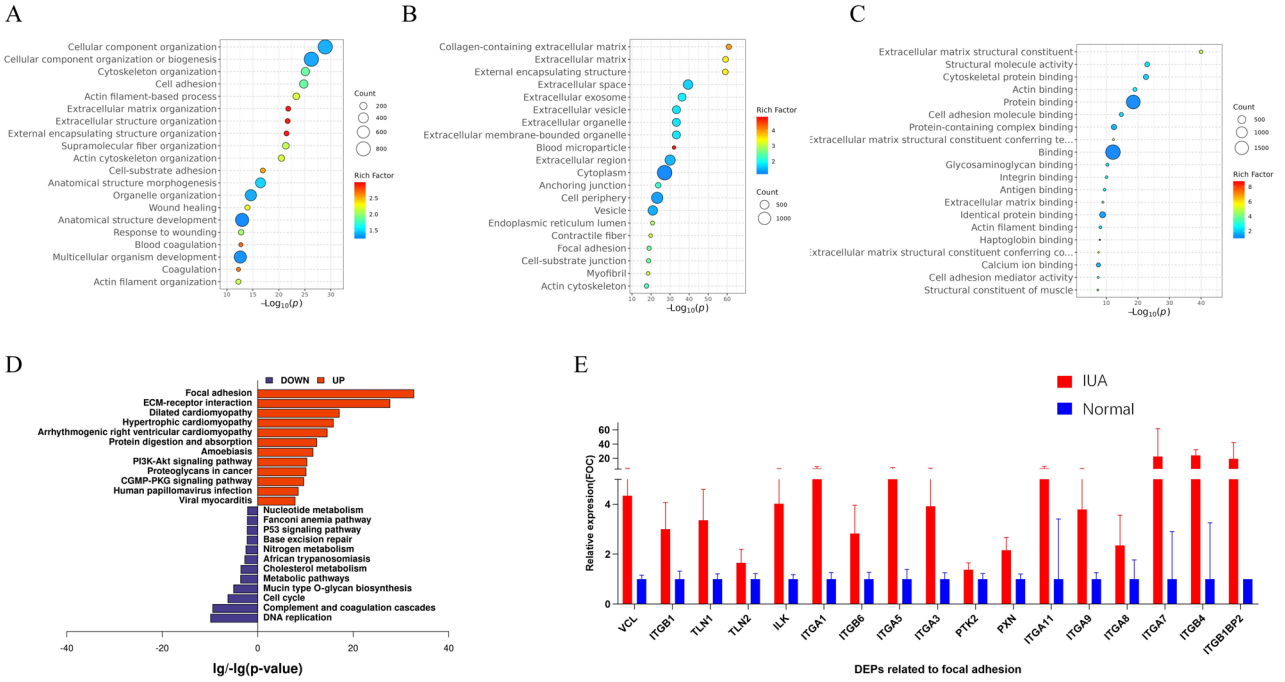

Fig. 4 GO and KEGG enrichment analysis of DEPs. GO enrichment in (**A)** Biological Process, **B** Cellular Component, and (**C)** Molecular Function. Dot size represents gene count; color indicates P-value. **D** Butterfly plot of KEGG pathways enriched by up-regulated (red) and down-regulated (blue) DEPs. **E** Expression levels of focal adhesion-related DEPs in IUA vs. control groups

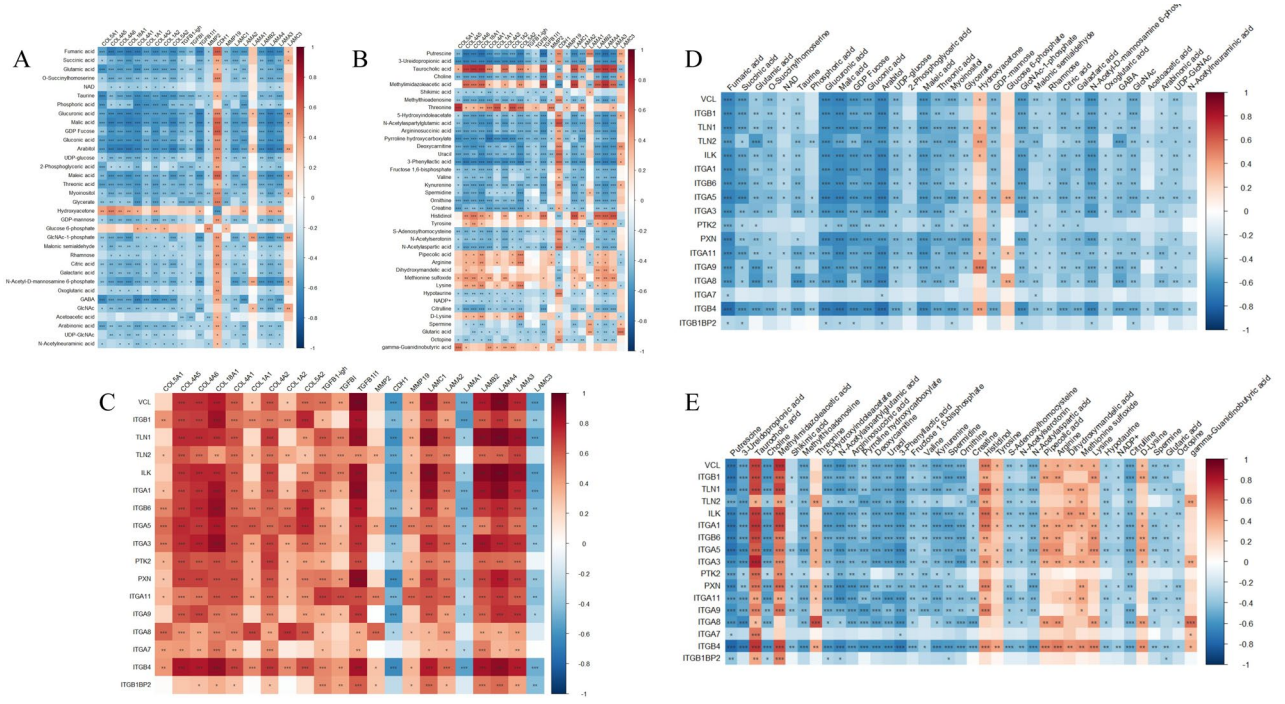

Fig. 5 Correlation heatmaps between metabolites and proteins (**A**) Glucose metabolism-related DEMs vs. fibrosis-related DEPs. **B** Amino acid metabolism-related DEMs vs. fibrosis-related DEPs. **C** Focal adhesion-related DEPs vs. fibrosis-related DEPs. **D** Focal adhesion-related DEPs vs. glucose metabolism-related DEMs. **E** Focal adhesion-related DEPs vs. amino acid metabolism-related DEMs. Red: positive correlation; blue: negative correlation. Asterisks indicate correlation significance (*$P < 0.05$, **$P < 0.01$, ***$P < 0.001$)

phosphorylation towards glycolysis, a pattern observed in various fibrotic diseases. This phenomenon aligns with the "Warburg effect" observed in various fibrotic diseases. For instance, ceria nanoparticles can alleviate fibrosis by inhibiting the key glycolytic enzyme HK2 [24]; while in myocardial fibrosis, inhibiting PFKFB3-mediated glycolysis effectively blocks Endothelial-Mesenchymal Transition (EndMT) and collagen deposition [25]. Although this study did not detect lactate, previous reports note that lactate enhances collagen stability and activates TGF-β1 signaling to promote fibroblast-to-myofibroblast transition, thus playing an important role in fibrosis [26]. Interestingly, although lipids and lipid-like molecules constituted the largest chemical category of DEMs, KEGG pathway enrichment analysis revealed that these lipid metabolites were predominantly enriched in pathways related to carbohydrate metabolism and amino acid metabolism, rather than in classical lipid metabolism pathways such as glycerophospholipid metabolism or fatty acid degradation. This pattern suggests that lipid alterations in IUA may primarily reflect their roles as signaling molecules or metabolic intermediates interfacing with central carbon and nitrogen metabolism, rather than representing primary disturbances in lipid biosynthetic or degradative pathways. For instance, glycerophospholipids can generate diacylglycerol and phosphatidic acid, which modulate insulin signaling and glucose uptake; sphingolipids such as ceramide influence glycolysis and insulin resistance; and fatty acid oxidation directly supplies acetyl-CoA to the TCA cycle. Therefore, while lipid molecules are numerically abundant among DEMs, their functional impact in IUA pathogenesis may be mediated through interactions with carbohydrate and amino acid metabolic networks.

Furthermore, proteomics analysis identified 2763 DEPs, with 801 upregulated and 1962 downregulated. Bifunctional enrichment analysis revealed that these proteins are primarily involved in processes such as extracellular matrix organization, cell adhesion, and cytoskeleton organization. KEGG pathway analysis further indicated significant activation of the Focal adhesion pathway in IUA, with increased expression of integrin family members (e.g., ITGB1, ITGA5, ITGA11) and focal adhesion-related molecules (e.g., FAK, Paxillin, Vinculin). Focal adhesions, as key hubs for cells to perceive mechanical and chemical signals from the microenvironment, participate in fibrosis regulation through multiple pathways. Yang et al. reported that nintedanib alleviates pulmonary fibrosis by inhibiting the FAK/ERK/S100A4 pathway [27]; Chen et al. further demonstrated that inhibiting the NLRP3 inflammasome reduces epithelial-mesenchymal transition (EMT) by downregulating FAK, thereby mitigating pulmonary fibrosis [28]. Additionally, Zyxin, a focal adhesion component, can promote skin fibrosis via integrin-mediated FAK/PI3K/AKT and TGF-β signaling pathways [29]. These results collectively suggest that focal adhesions have been implicated in various fibrotic diseases based on prior functional studies, although their role in gynecological conditions, particularly IUA, remains understudied. Takashi Nagai et al. found that both FAK and MCP-1 expression were upregulated in fibrotic tissues of endometriosis, and inhibiting FAK reduced TGF-β1 and inflammatory cytokine expression, alleviating fibrosis [30], suggesting FAK exerts regulatory functions in uterine-related fibrosis.

Integrated metabolite-protein analysis revealed that glucose and amino acid metabolism-related DEMs generally correlated negatively with fibrosis-related DEPs, whereas focal adhesion-related DEPs correlated positively with fibrosis DEPs. Most importantly, glucose and amino acid metabolism-related DEMs also showed significant negative correlations with focal adhesion-related DEPs, suggesting potential functional interaction between metabolic reprogramming and focal adhesion signaling in IUA fibrosis. Studies have shown [31] that specific amino acids (e.g., tyrosine, phenylalanine, methionine) can inhibit integrin expression and FAK phosphorylation, affecting tumor cell attachment and spreading; whereas in hepatic stellate cells, integrins regulate their activation and fibrosis formation via the Hippo pathway [32]. These results support the notion that metabolite changes can directly influence focal adhesion function, thereby regulating cell phenotype. Downstream of focal adhesions, the PI3K-AKT signaling pathway was also significantly activated in IUA tissues. This pathway, a key regulatory axis in fibrosis formation, participates in various biological processes including metabolism, autophagy, and EMT. Hu et al. showed that lipopolysaccharide promotes glycolysis in lung fibroblasts by activating the PI3K-AKT-mTOR/PFKFB3 pathway, thereby exacerbating pulmonary fibrosis [33]; Guo et al. found that β-Klotho is highly expressed in the basal endometrium of IUA patients and promotes fibrosis via the PI3K-AKT pathway [34]; and Zhang et al. reported that estrogen-loaded Heparin-poloxamer microspheres enhance their therapeutic efficacy for IUA by inhibiting the PI3K-AKT pathway [35]. These studies consistently indicate the core role of the PI3K-AKT pathway in fibrosis across different tissues.

Based on integrated multi-omics correlation analyses and literature evidence, we propose the following working hypothesis to guide future investigations: Following endometrial basal layer injury, impaired local microvascular regeneration may lead to inadequate blood supply and hypoxia, potentially triggering metabolic reprogramming characterized by enhanced glycolysis and disordered amino acid metabolism [36]. Some metabolites (e.g., proline, hydroxyproline) directly participate in collagen synthesis, altering the composition and

mechanical properties of the extracellular matrix (ECM). These ECM changes are transmitted intracellularly via integrin-focal adhesion signaling, activating the FAK/PI3K/AKT/mTOR pathway, which in turn suppresses autophagy, promotes EMT and collagen deposition, ultimately leading to fibrosis. Furthermore, mTOR, acting as a metabolic sensing hub, can respond to intracellular energy and metabolite changes: for instance, decreased α-ketoglutarate weakens its role in promoting autophagy and antioxidant stress; declining ATP levels inhibit AMPK, relieving its suppression of mTOR and further activating mTOR signaling; under hypoxic conditions, mTORC1 can also enhance HIF-1α protein translation, upregulating glycolytic enzymes and glucose transporters, thereby promoting glycolysis. This putative positive feedback loop, if functionally validated, could contribute to the progression of fibrosis in IUA.

It is important to emphasize that the proposed mechanistic model is derived from correlational data and represents a hypothesis-generating framework rather than a validated pathway. The observed associations between metabolites and proteins, while statistically significant, do not establish causality. Functional experiments—such as FAK inhibition, integrin knockdown, or glycolysis modulation in endometrial fibroblasts or organoid models—are essential to test whether the integrin-focal adhesion signaling pathway indeed drives fibrosis through interaction with metabolic reprogramming.

Several limitations of this study should be acknowledged. First, while the integrated multi-omics approach provides a comprehensive overview of molecular alterations in IUA, the cross-sectional design precludes causal inferences. The proposed mechanistic relationships—including the integrin-focal adhesion-FAK/PI3K/AKT/mTOR positive feedback loop—are constructed from correlation networks and literature extrapolation rather than direct experimental evidence. No in vitro or in vivo functional validation (e.g., FAK inhibition, integrin knockdown, glycolysis modulation in endometrial fibroblasts or organoids) was performed. Therefore, the mechanistic model should be interpreted as a hypothesis-generating framework requiring rigorous experimental testing. Second, although 55 clinical samples represent a reasonable cohort for exploratory omics studies, the sample size remains relatively modest. Individual variability in metabolic and protein profiles may influence the results, and the findings should be validated in larger, multi-center cohorts to enhance generalizability. Third, this study lacked an independent validation cohort for both metabolomic and proteomic discoveries. Independent replication using additional patient samples would strengthen the robustness of the identified differentially expressed metabolites and proteins. Fourth, the tissue samples analyzed in this study were derived from bulk endometrial biopsies, which contain heterogeneous cell populations including epithelial cells, fibroblasts, immune cells, and vascular components. As a result, the observed molecular signatures represent an average across cell types and may obscure cell-type-specific contributions to fibrosis. Future studies employing single-cell or spatial omics technologies could provide deeper insights into the cellular heterogeneity of the fibrotic microenvironment. Fifth, the control group comprised patients with tubal factor infertility or uterine cesarean scar diverticulum rather than healthy fertile women, due to ethical constraints in obtaining endometrial tissue from asymptomatic individuals. Although all control samples were pathologically confirmed to have no endometrial lesions, we cannot completely exclude the possibility that these underlying conditions might subtly influence the endometrial metabolome or proteome. Future studies should ideally include multiple control groups or validate key findings in independent cohorts when ethically permissible. Finally, while the integration of metabolomics and proteomics revealed significant correlations between metabolic pathways and fibrosis-related proteins, the functional consequences of these correlations remain to be elucidated. Targeted metabolic interventions or genetic modulation of key molecules in experimental models will be necessary to establish causative roles. Despite these limitations, the present study provides a valuable resource for understanding the molecular landscape of IUA-associated fibrosis and offers multiple hypotheses for future mechanistic and therapeutic investigations. To address this, future studies should include: (1) in vitro experiments using primary endometrial cells treated with key metabolites (e.g., fumarate, arginine) or FAK inhibitors to assess effects on collagen synthesis and integrin signaling; (2) in vivo validation using IUA animal models with targeted interventions such as glycolysis modulators (e.g., 2-DG) or focal adhesion pathway inhibitors, followed by histological assessment of fibrosis severity.

Conclusion

In conclusion, the pathogenesis of IUA fibrosis is associated with concurrent alterations in metabolic profiles, focal adhesion signaling, and the PI3K-AKT-mTOR pathway. These correlational findings provide a rationale for future studies to investigate causal relationships and therapeutic targeting of these interconnected pathways. While the correlational findings from this multi-omics study provide a comprehensive molecular map and generate testable hypotheses, future studies must focus on functional validation of key omics-identified molecules within this fibrotic network. Such causal evidence is essential to lay a theoretical foundation for developing novel interventions targeting the metabolic-signaling network hubs.

Abbreviations

AFS	American Fertility Society
BP	Biological Process
CC	Cellular Component
DEMs	Differentially expressed metabolites
DEPs	Differentially expressed proteins
ECM	Extracellular matrix
EMT	Epithelial-mesenchymal transition
GO	Gene Ontology
IUA	Intrauterine adhesions
MF	Molecular Function
PVO	Prunella vulgaris oil
TCRA	Transcervical Resection of Adhesions

Authors' contributions

Shuhan He: Data curation, Investigation, Methodology, Writing – original draft. Hui Yuan: Data curation, Methodology, Writing – review & editing. Xingping Zhao: Conceptualization, Data curation, Investigation, Methodology, Funding acquisition, Writing – original draft. Enuo Peng: Data curation, Investigation. Dabao Xu: Data curation, Supervision, Writing – review & editing. Aiqian Zhang: Data curation, Project administration, Supervision, Validation, Funding acquisition, Writing – review & editing. All authors approved the final version of the manuscript.

Funding

This study was supported by grants from Provincial Natural Science Foundation of Hunan (2025JJ50518) and Health Commission of Hunan Province (20255960).

Data availability

The data that support the findings of this study are available from the corresponding author upon reasonable request.

Declarations

Ethics approval and consent to participate

This study was performed in accordance with the Declaration of Helsinki and approved by the Ethics Committee of the Third Xiangya Hospital (Approval No. Kua 24558). All participants gave informed consent.

Competing interests

The authors declare no competing interests.

Author details

[1]Department of Gynecology, Third Xiangya Hospital of Central South University, 138 Tongzipo Road, Changsha, Hunan 410013, China
[2]Clinical Research Center, Clinical Postdoctoral Research station, the Third Xiangya Hospital, Central South University, 138 Tongzipo Road, Changsha, Hunan 410013, China

Received: 27 December 2025 / Accepted: 16 March 2026
Published online: 11 April 2026

References

1. Zhao G, Hu Y. Mechanistic insights into intrauterine adhesions. Semin Immunopathol. 2024;47(1):3.
2. Lee W-L, Liu C-H, Cheng M et al. Focus on the primary prevention of intrauterine adhesions: current concept and vision. Int J Mol Sci, 2021, 22(10).
3. Wang P-H, Yang S-T, Chang W-H, et al. Intrauterine adhesion. Taiwan J Obstet Gynecol. 2024;63(3):312–9.
4. Zhu H, Li T, Xu P et al. Effect of autologous bone marrow stem cells-scaffold transplantation on the ongoing pregnancy rate in intrauterine adhesion women: a randomized, controlled trial. Sci China Life Sci, 2023.
5. Hooker AB, de Leeuw RA, Twisk JWR, et al. Reproductive performance of women with and without intrauterine adhesions following recurrent dilatation and curettage for miscarriage: long-term follow-up of a randomized controlled trial. Hum Reprod. 2021;36(1):70–81.
6. Ma J, Zhan H, Li W, et al. Recent trends in therapeutic strategies for repairing endometrial tissue in intrauterine adhesion. Biomater Res. 2021;25(1):40.
7. Liu X, Zhang X, Hua K. Hysteroscopic surgery for intrauterine scar adhesions after laparoscopic metroplasty in a patient with a unicornuate uterus and a functional noncommunicating rudimentary horn. Gynecol Minim Invasive Ther. 2024;13(3):202–3.
8. Zhang J, Shi C, Sun J, et al. Analysis of factors affecting the prognosis of patients with intrauterine adhesions after transcervical resection of adhesions. Fertil Steril. 2024;122(2):365–72.
9. Zhao J, Zhang L, Liang J, et al. The effect of the combined use of an intrauterine device and a Foley balloon in the prevention of adhesion following hysteroscopic adhesiolysis. Women Health. 2022;63(1):1–7.
10. Sun Y, Chen X, Qian Z, et al. Estradiol and intrauterine device treatment for moderate and severe intrauterine adhesions after transcervical resection. BMC Womens Health. 2022;22(1):357.
11. Luo Y, Sun Y, Huang B et al. Effects and safety of hyaluronic acid gel on intrauterine adhesion and fertility after intrauterine surgery: a systematic review and meta-analysis with trial sequential analysis of randomized controlled trials. Am J Obstet Gynecol, 2024, 231(1).
12. Yu J, Zhang W, Huang J, et al. Management of intrauterine adhesions using human amniotic mesenchymal stromal cells to promote endometrial regeneration and repair through Notch signalling. J Cell Mol Med. 2021;25(23):11002–15.
13. Cao C, Zhou Q, Hu Z, et al. A retrospective study of estrogen in the pretreatment for medical management of early pregnancy loss and the inference from intrauterine adhesion. Eur J Med Res. 2022;27(1):129.
14. Song Y-T, Liu P-C, Tan J, et al. Stem cell-based therapy for ameliorating intrauterine adhesion and endometrium injury. Stem Cell Res Ther. 2021;12(1):556.
15. Liu L, Yan S, Qiu T, et al. Study on the endometrial metabolomics of intrauterine adhesions. Progress Obstet Gynecol. 2022;31(7):521–5.
16. Li L, Deng J, Lin L-M, et al. Metabolomics and pharmacodynamic analysis reveal the therapeutic role of Prunella vulgaris oil on intrauterine adhesion rats. J Pharm Biomed Anal. 2022;209:114532.
17. Rozanova S, Barkovits K, Nikolov M et al. Quantitative Mass Spectrometry-Based Proteomics: An Overview. Methods Mol Biol. 2021;2228.
18. Horn P, Tacke F. Metabolic reprogramming in liver fibrosis. Cell Metab. 2024;36(7):1439–55.
19. Tang K, Zhang H, Deng J, et al. Ammonia detoxification promotes CD8 + T cell memory development by urea and citrulline cycles. Nat Immunol. 2023;24(1):162–73.
20. Elmetwally MA, Li X, Johnson GA, et al. Dietary supplementation with L-arginine between days 14 and 25 of gestation enhances NO and polyamine syntheses and the expression of angiogenic proteins in porcine placentae. Amino Acids. 2021;54(2):193–204.
21. Zhang Y, Shi L, Lin X, et al. Unresponsive thin endometrium caused by Asherman syndrome treated with umbilical cord mesenchymal stem cells on collagen scaffolds: a pilot study. Stem Cell Res Ther. 2021;12(1):420.
22. Varghese N, Werner S, Grimm A et al. Dietary Mitophagy Enhancer: A Strategy for Healthy Brain Aging? Antioxid (Basel). 2020;9(10).
23. Li J-M, Yang DC, Oldham J, et al. Therapeutic targeting of arginino-succinate synthase 1 (ASS1)-deficient pulmonary fibrosis. Mol Ther. 2021;29(4):1487–500.
24. Wang M, Zeng F, Ning F, et al. Ceria nanoparticles ameliorate renal fibrosis by modulating the balance between oxidative phosphorylation and aerobic glycolysis. J Nanobiotechnol. 2022;20(1):3.
25. Zeng H, Pan T, Zhan M, et al. Suppression of PFKFB3-driven glycolysis restrains endothelial-to-mesenchymal transition and fibrotic response. Signal Transduct Target Ther. 2022;7(1):303.
26. Song S, Wu S, Meiduo D, et al. Nano-biomaterial Fibrinogen/P(LLA-CL) for prevention of intrauterine adhesion and restoration of fertility. J Biomed Mater Res A. 2024;112(2):167–79.
27. Yang W, Pan L, Cheng Y et al. Nintedanib alleviates pulmonary fibrosis in vitro and in vivo by inhibiting the FAK/ERK/S100A4 signalling pathway. Int Immunopharmacol. 2022;113(Pt A):09409.
28. Chen W-C, Yu W-K, Su V, Y-F et al. NLRP3 Inflammasome Activates Endothelial-to-Mesenchymal Transition via Focal Adhesion Kinase Pathway in Bleomycin-Induced Pulmonary Fibrosis. Int J Mol Sci. 2023;24(21).
29. Huang Y, Zhao H, Zhang Y, et al. Enhancement of Zyxin Promotes Skin Fibrosis by Regulating FAK/PI3K/AKT and TGF-β Signaling Pathways via Integrins. Int J Biol Sci. 2023;19(8):2394–408.
30. Nagai T, Ishida C, Nakamura T, et al. Focal Adhesion Kinase-Mediated Sequences, Including Cell Adhesion, Inflammatory Response, and Fibrosis, as a Therapeutic Target in Endometriosis. Reprod Sci. 2020;27(7):1400–10.

31. Chang HN, Chen CK, Yu TY, et al. Lidocaine inhibits migration of tenocytes by downregulating focal adhesion kinase and paxillin phosphorylation. J Orthop Res. 2024;42(5):985–92.
32. Kitsugi K, Noritake H, Matsumoto M, et al. Arg-Gly-Asp-binding integrins activate hepatic stellate cells via the hippo signaling pathway. Cell Signal. 2022;99:110437.
33. Hu X, Xu Q, Wan H, et al. PI3K-Akt-mTOR/PFKFB3 pathway mediated lung fibroblast aerobic glycolysis and collagen synthesis in lipopolysaccharide-induced pulmonary fibrosis. Lab Invest. 2020;100(6):801–11.
34. Guo Z, Wang Y, Wen X et al. β-Klotho Promotes the Development of Intrauterine Adhesions via the PI3K/AKT Signaling Pathway. Int J Mol Sci. 2022;23(19).
35. Zhang S-S, Xia W-T, Xu J, et al. Three-dimensional structure micelles of heparin-poloxamer improve the therapeutic effect of 17β-estradiol on endometrial regeneration for intrauterine adhesions in a rat model. Int J Nanomed. 2017;12:5643–57.
36. Zhu Z, Zhang Y, Zhang Y, et al. Exosomes derived from human umbilical cord mesenchymal stem cells accelerate growth of VK2 vaginal epithelial cells through MicroRNAs in vitro. Hum Reprod. 2019;34(2):248–60.

Publisher's note